Modelling of two damaged unreinforced masonry buildings following the Canterbury earthquakes

S. Marino, S. Cattari & S. Lagomarsino

University of Genoa, Genoa, Italy.

J.M. Ingham & D. Dizhur

University of Auckland, Auckland, New Zealand.

2016 NZSEE Conference

ABSTRACT: The reported study focused on modelling the seismic response of two URM buildings that were damaged in the Canterbury earthquake sequence. Static and dynamic nonlinear analyses were undertaken using the equivalent frame approach. Actual time-history records attained during the earthquakes where used to undertake dynamic analyses and facilitate direct comparison to the observed building damage. The results showed that use of the equivalent frame method enabled prediction of the seismic response of the two case study buildings with a high level of accuracy.

1 INTRODUCTION AND MOTIVATIONS

Following the 2010/2011 Canterbury earthquakes there has been renewed focus on assessing the earthquake capacity of existing unreinforced masonry (URM) buildings, with this need being legislated with the earthquake prone buildings amendments bill to the Building Act 2004 (Amendment Bill, 2013 No 182-1). In the reported study, the attention was focused on the global response of URM buildings, where it was assumed that appropriate connections exist between structural elements that prevent the activation of local failure modes, mainly associated with the out-of-plane response of walls. Within this context, the global seismic response is related both to the in-plane capacity of walls and to the load transfer via floor and roof diaphragms. There are a number of different possible modelling strategies available in literature and in various codes, standards and guidelines. The focus of the study reported herein was on using the equivalent frame (EF) approach with a purposely developed software, Tremuri (Lagomarsino et al. 2013). In the EF approach, each load resisting URM element is subdivided into a set of URM panels (where the deformation and the nonlinear response are concentrated), and a companion set of rigid portions or joints, which connect the URM panels. The EF approach requires a limited number of degrees of freedom, and allows nonlinear dynamic analyses of complex three dimensional models of URM structures to be undertaken with a reasonable computational effort. Moreover the idealisation of the structural system as an EF allows the introduction of other elements, such as reinforced concrete, steel or wooden beams and columns.

The use of the EF approach is proposed in NZSEE (2015) along with a worked example on a case study prototypical New Zealand URM building (Cattari et al. 2015, EQ STRUCT 2015). The case study URM building was damaged in the 2007 Gisborne earthquake and good correlation of the actual vs predicted performance was shown using the EF approach. Further research was initiated to investigate the reliability of this procedure by attempting to simulate the observed seismic response of two additional case study URM buildings that were damaged during the Canterbury earthquake sequence. These two case study buildings are: (1) Avonmore House (AH) that was located at 203 Hereford Street in Christchurch and (2) Royal Hotel (RH) that was located at 34 Norwich Quay in Lyttelton (Fig. 1). The two case study buildings were standalone structures and exhibited a clearly prevailing in-plane global response during the earthquake induced shaking, and hence were selected as suitable exemplar cases for investigating the reliability of an EF approach. AH and RH were significantly damaged during the Canterbury earthquake and were subsequently demolished. Prior and during the building demolition, sustained damage was well documented and a detailed photographic record was collected. In addition, construction and alteration drawings were acquired from Christchurch City Council records property files and were reviewed in detail.

a) Avonmore House

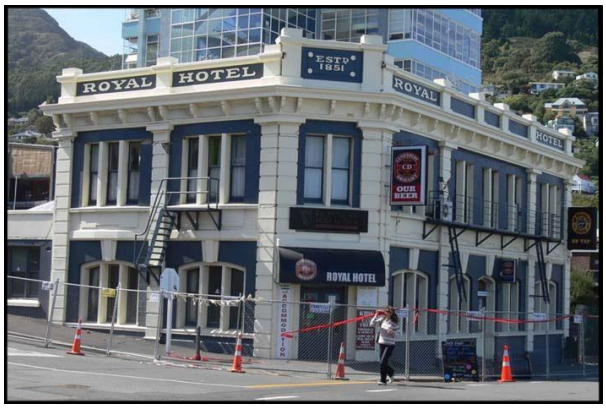

b) The Royal Hotel

Figure 1 - Illustrations of the subject buildings

(photographs taken following the 22 February 2011 earthquake)

2 DESCRIPTION OF CASE STUDY BUILDINGS

Figure 2 shows a plan view of both subject buildings, together with a 3D view of their geometrical configuration.

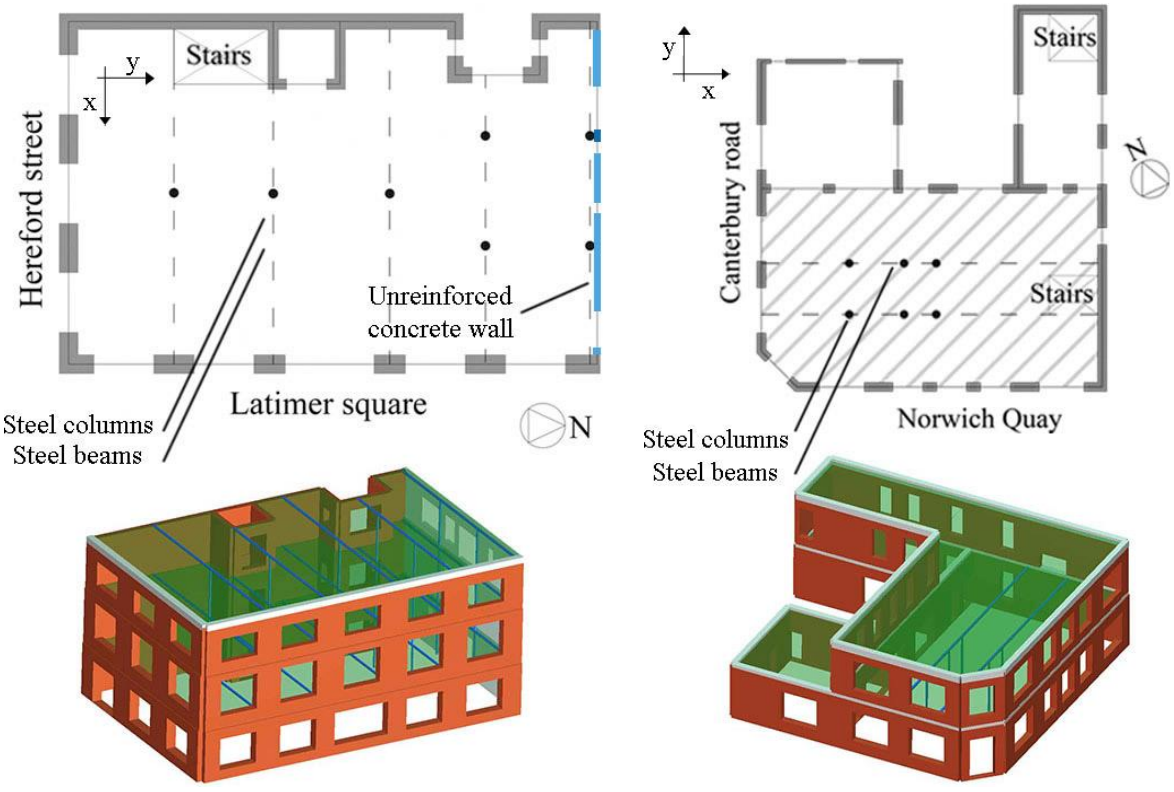

a) Ground floor plan and Tremuri 3D model of AH

b) Ground floor plan and Tremuri 3D model of RH (hatched area explained in Section 2.2)

Figure 2 - General layout and geometry of the subject buildings

Table 1. Approximated wall characteristics of the case study buildings

	Element	Ground floor	First floor	Second floor
AH	Wall thickness (mm)	710 (6 leaves)	590 (5 leaves)	470 (leaves)
	Inter-storey height (m)	3.70	3.95	3.50
RH	Wall thickness (mm)	470 (4 leaves)	350 (3 leaves)	-
	Inter-storey height (m)	3.57	3.60	-

2.1 **Avonmore House**

AH was a three storey building with external clay brick URM walls on three sides and an unreinforced concrete wall on the North side. The timber floor diaphragms were supported by the external walls and on internal steel frames. AH was a standalone structure located on sand and silty-sand soil that is at least 23 m deep (from borehole data). The building presented a significant plan irregularity due to the heavily perforated South and the East façades, whereas the West façade was an unperforated masonry wall with additional stiffness provided by the URM return walls of the elevator that were four leaves in thickness (470 mm). The North wall consisted of unreinforced concrete and was assumed to be non-loadbearing due to evidence of a loadbearing independent steel frame supporting the floor gravity loads in the vicinity. The North wall was initially an unperforated unreinforced concrete wall, with openings subsequently added as part of alterations during the lifetime of the building with an RC lintels installed above these openings. AH was approximately 11.2 m high (excluding parapets) with a plan area of approximately 380 m^2. The thicknesses of the walls were estimated from photographic evidence collected during the demolition, and are summarised in Table 1. Each timber floor and roof diaphragm spanned between perimeter URM walls and had intermediate support provided by seven internal steel columns located underneath steel beams that are thought to have been 500 mm high (shown dashed in Fig. 2). The parapet height was estimated to be 2.5 m on the South and East façades and 1.2 m on the North and West façades, with all parapets being four leaves in thickness (470 mm). On the South and East façades concrete ring beams were assumed to consist of 3 bars of ¾ inches (approximately 19 mm) longitudinal reinforcement, without transverse reinforcement. A lightweight partial extension on the roof level was not modelled in the equivalent frame model, and only its weight was considered.

The AH building had undergone seismic retrofitted in 1994 where each of the floor diaphragms were overplyed with 20 mm particleboard. Perimeter URM walls were connected to the floor and roof diaphragms using a combination of adhesive anchors and steel equal angels. Furthermore, the floor and roof diaphragms were fixed to the unreinforced concrete North wall. For this reason, a higher value for the shear stiffness of the diaphragms was used than suggested in the NZSEE (2015) guidelines (Table 3). Steel parapet restraints were also added at the roof level around the building perimeter.

2.2 **Royal Hotel**

The Royal Hotel (RH) was a two storey building with external clay brick URM walls, internal steel frames (likely only at ground floor) and timber floors. The building was approximately 7.2 m high (excluding the parapets) with a plan area approximated as 290 m^2 at ground floor and 250 m^2 at 1st floor (excluding small rooms on ground floor that were added following subsequently construction). Drawings showing wall thicknesses were not available, and the dimensions were estimated based on limited photographs that were taken during building demolition. The assumed dimensions are reported in Table 1. The timber floor diaphragms spanned between perimeter URM walls and, at least at ground floor, they had intermediate support provided by two internal steel frames (shown dashed in Fig. 2).

The parapet height was estimated as 1.2 m above the part of the building shown hatched in Figure 2b and 1.0 m on the remaining part, with both sections being 3 leaves in thickness (350 mm). Based on photographic evidence, concrete ring beams were identified at the ground and first floor levels. Evidence of steel reinforcement was only identified for the concrete ring beam located on the first

level and based on observed earthquake damage it was assumed that reinforcement was also present in the ground floor ring beam.

2.3 **Loads, seismic weight and material properties**

Table 2 provides the assumed permanent and imposed load applied to AH and RH.

Table 2. Adopted loads for the subject buildings

Element	Description	Permanent load	Imposed load
Timber floors and roof diaphragm	Framing, floorboard and ceiling. Superimposed dead load from services	0.5 kPa	0.65 kPa
Clay brick masonry	External loadbearing walls	18 kN/m^3	Not applicable
Concrete elements	Ring beams at each storey	25 kN/m^3	Not applicable
Internal partitions	Timber stud framing, plasterboard lining	0.65 kPa	Not applicable

For AH, the mortar compressive strength (18 MPa) was determined using samples extracted from the building during demolition, with the results of those tests having been reported in Lumantarna (2012). For cohesion and friction the values suggested in NZSEE (2015) for cement based mortars were used. Tests on the bricks were not carried out, but based on surveys made during the building demolition, the bricks were deemed to be strong and difficult to scratch. Based on these observations and the recommendations in NZSEE (2015), an average brick compression strength of 26 MPa was adopted. In order to establish the: (i) probable masonry compressive strength, (ii) the masonry Young's Modulus and (iii) the masonry shear modulus, the equations proposed in NZSEE (2015) were used and the results are reported in Table 3. However for the masonry Young's Modulus a values of 500 times the masonry compressive strength instead of 300 times was used because for the case of strong cement mortars this value better matched the value suggested in EN 1998-1. Material tests were not carried out for RH. From the photographs and site observations that were made during site inspection following the earthquakes, the bricks appeared soft and it was identified that lime mortar was used in the original construction. The procedure outlined in NZSEE 2015 was used for estimating the material propertied for such characteristics (reported in Table 3).

Table 3. Summary of the mechanical properties used in the assessment

	Masonry properties		**Diaphragms properties**	
AH	Young's modulus*	10.28 GPa	Young's modulus in the joist direction	22.5 GPa
	Shear modulus*	4.11 GPa	Young's modulus in the direction perpendicular to E_1	10 GPa
	Compressive strength	20.55 MPa	Shear modulus	875 MPa
	Brick tensile strength	3.1 MPa	Thickness	40 mm
	Cohesion**	0.63 MPa		
RH	Young's modulus*	2.01 GPa	Young's modulus in the joist direction	22.5 GPa
	Shear modulus*	0.80 GPa	Young's modulus in the direction perpendicular to E_1	10 GPa
	Compressive strength	6.68 MPa	Shear modulus	87.5 MPa
	Brick tensile strength	1.7 MPa	Thickness	40 mm
	Cohesion**	0.28 MPa		

*Values of the cracked stiffness. The initial stiffness was assumed to be double this value.

**The values of the cohesion were modified according to the Mann and Muller proposal (1980).

2.4 **Basis of equivalent frame model**

The seismic response of the case study buildings was simulated by performing nonlinear analyses through the adoption of the Equivalent Frame (EF) modelling strategy that is based on discretisation of the walls into a set of masonry panels (piers and spandrels), in which the nonlinear response is concentrated, connected by rigid areas (nodes). The EF analysis was performed using the Tremuri software (Lagomarsino et al. 2013). It is highlighted that only the in-plane response was considered, recognising that apart from a small portion of the parapet, no out-of-plane collapse occurred in either building during the Canterbury earthquakes. The nonlinear response of masonry panels was modelled by adopting nonlinear beams with a multilinear constitutive law that was recently implemented in the software used (Cattari & Lagomarsino 2013). The elastic response phase is described according to beam theory by defining the initial Young's (E) and shear (G) moduli of masonry, and then the progressive degradation is approximated using a secant stiffness (the values defined in Table 3). The elastic values are defined by multiplying the secant stiffness by a coefficient, in this case equal to 2 (as suggested in EN 1998-1). The maximum shear strength is defined on the basis of common criteria proposed in literature as a function of different failure modes examined (either flexural or shear). The progression of nonlinear response is defined through subsequent strength decay (β_{Ei}) and drift limits (δ_{Ei}), which are associated with the achievement of reference damage levels (DLi with i=1,5, where DL5 is associated with "collapse" of the panel, representing as the state when the panel has lost the capacity to support horizontal loads) as shown in Fig. 3a and Table 4. Moreover, an accurate description of the hysteretic response is also included based on a phenomenological approach that is able to account for the typical response of panels having a prevailing shear or flexural behaviour (Fig. 3). Mixed failure modes are also taken into account and parameters may be calibrated in order to differentiate between the behaviour of piers and spandrels. In case of openings with URM arches, a depth up to 2/3 of the radius of the arches was used for the beams of the EF. In the multilinear constitutive law the shear decays correspond to drift values derived from experimental evidences of spandrels with URM arches underneath (Beyer 2012). For their flexural behaviour an equivalent tensile strength contribution was considered as adopted in NZSEE (2015) and proposed in Beyer (2012). Finally, diaphragms are modelled as horizontal orthotropic membrane finite elements.

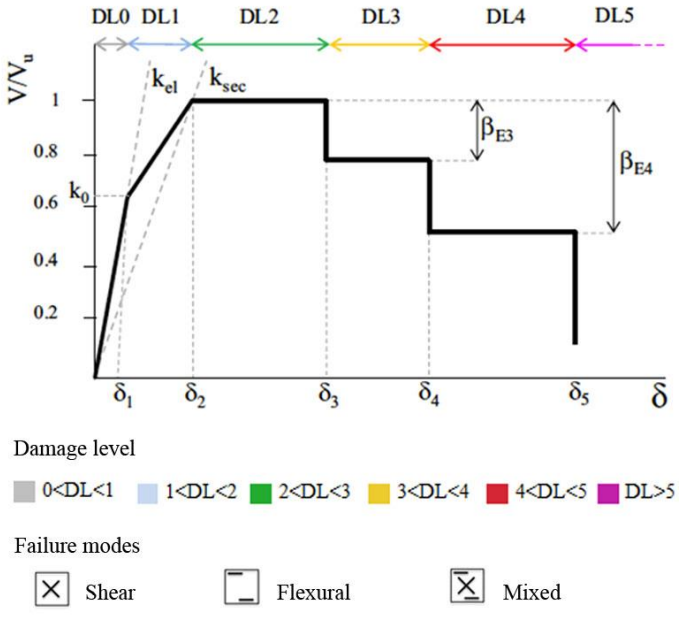

a) Backbone response of a masonry panel and definition of the associated colours and symbols (adapted from Cattari and Lagomarsino 2013)

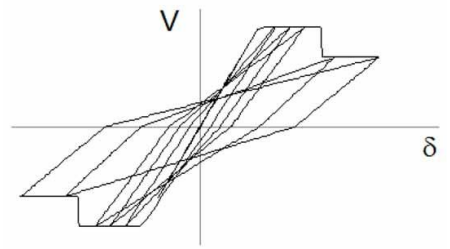

b) Example of hysteretic response for the case of a shear failure mode

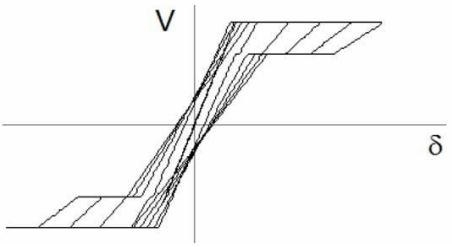

c) Example of hysteretic response for the case of a flexural failure mode

Figure 3 - Details of the multilinear constitutive law for a masonry panel

Table 4. Summary of the threshold used for piers and spandrels

[%]	δ_{E3}*	δ_{E4}*	δ_{E5}*	β_{E3}*	β_{E4}*
Piers**	0.6 - 0.3	0.8 - 0.5	1 - 0.7	0 - 15	30 - 60
Spandrels	0.2	0.6	2	50	50

*δ_{Ei} drift limits, β_{Ei} strength decays as shown in Figure 3a

**The first value is assumed in case of prevailing flexural behaviour, the second in case of shear

3 ANALYSIS OF THE DAMAGE AND NUMERICAL SIMULATIONS

Nonlinear time history analyses using the numerical models described above were carried out in order to simulate the seismic response of the case study buildings. Thanks to the New Zealand GeoNet project it was possible to identify two time history accelerograms recorded by stations located in the vicinity of the subject buildings. For AH the CCCC (Christchurch Cathedral College) strong motion record was used, that was recorded approximately 800 m distant from the building, whereas for RH the LPCC (Lyttelton Port Company) strong motion data was used that was recorded approximately 900 m distant (Fig. 4). For the recorded histories the values of the peak ground accelerations (PGA) are reported in Table 5. It is noted that the CCCC recording station is situated on a type of soil similar to the one where AH was located (Wotherspoon et al. 2015), whereas the LPCC station is instead situated on rock whilst RH was situated in the centre of the valley where the town of Lyttelton is built and therefore the case study building was expected to have at least 12 m of sediments underneath.

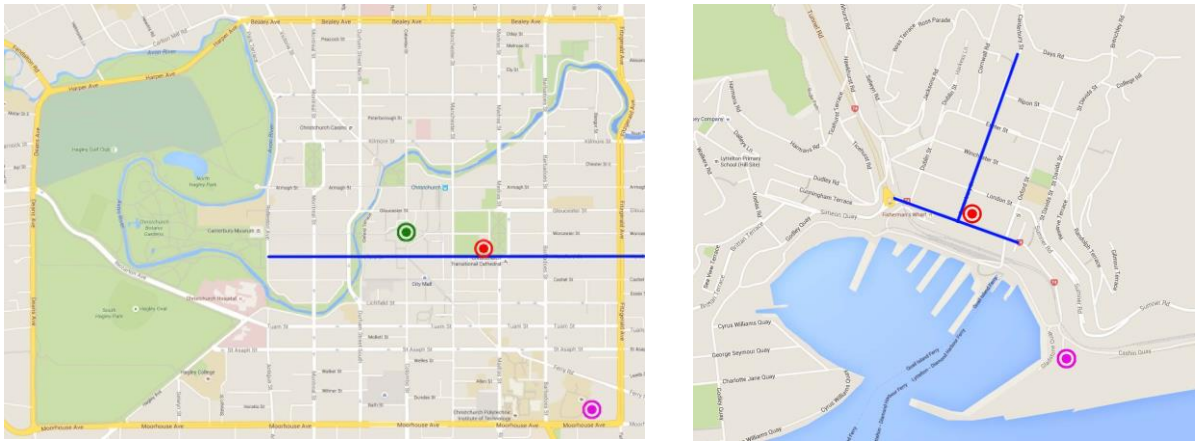

a) Circled in red the location of AH, in magenta the strong motion recorder and in green the Cathedral

b) Location of RH in Lyttelton (circled in red) and of the strong motion recorder (circled in magenta)

Figure 4 - Locations of case study buildings. The streets where the buildings were located are marked in light blue (images from Google)

In Figure 5 the comparison between the real damage to AH and the results of the simulation carried out with Tremuri is shown. In the simulation the model mainly presented spandrel damage, particularly on the South façade, and this finding is consistent with the damage observed in the building after the earthquake. Furthermore, in this façade (the shorter) it was also possible to identify wide cracks in the piers (mainly in the top storey) that the simulation was able to predict.

RH presented less extensive damage than AH, mainly concentrated in the piers. This observation supports the hypothesis that reinforcement was present in the ring beams. The numerical response, however, seemed to show an overall lower damage if compared with the response of the building during the earthquake. A possible explanation could be that the strong motion was recorded on a different type of soil, and therefore no particular site effect was accounted for. For the meaning of the colours and the symbol of the numerical model screenshots refer to Figure 3.

a) South façade of AH after the earthquake. Damage is evident in the spandrels and in the exterior and top piers

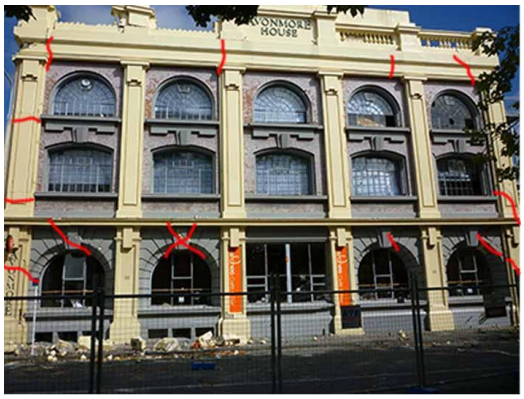

b) East façade of AH after the earthquake. Damage was mainly in the spandrels and external piers

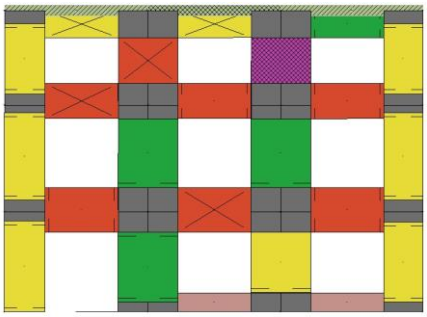

c) Damage in the South façade of the Tremuri model at the end of the dynamic analysis

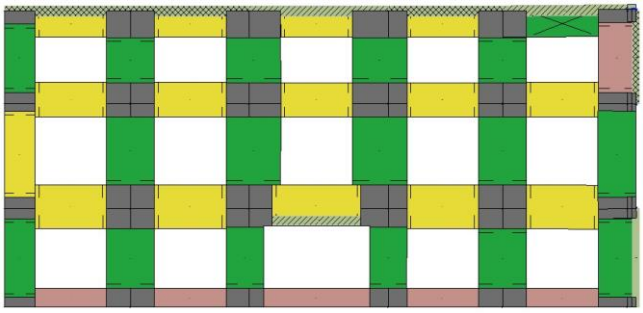

d) Damage in the East façade of the Tremuri model at the end of the dynamic analysis

Figure 5 - Comparison between the real damage and the numerical analysis for AH (in the East façade the cracks are highlighted in red for clarity). See Figure 3 for meaning of colours and symbols.

a) Façade of RH on Canterbury road. Cracks are highlighted in red for clarity

b) Façade of RH on Norwich Quay. Cracks are highlighted in red for clarity

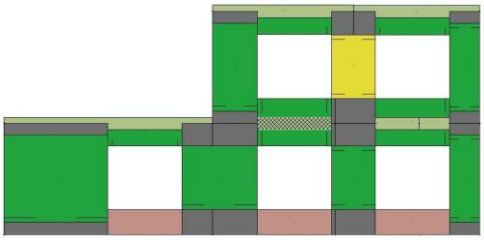

c) Tremuri damage forecast in the façade on Canterbury road at the end of the dynamic analysis

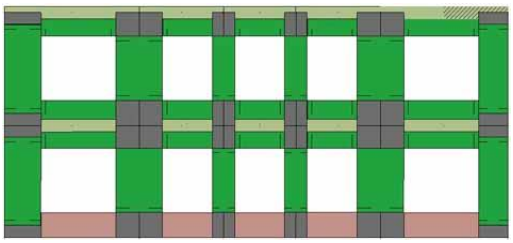

d) Tremuri damage forecast in the façade on Norwich Quay at the end of the dynamic analysis

Figure 6 - Comparison between the observed damage and the numerical analysis for RH (cracks are highlighted in red for clarity). See Figure 3 for meaning of colours and symbols.

In Figures 7 and 8 the comparisons between the results of nonlinear dynamic analyses and those of nonlinear static analyses are depicted. The red curves refer to analyses where the applied load pattern was proportional to the masses (rectangular acceleration profile), and the blue curves refer to the analyses where an inverted triangular acceleration profile was assumed. On the vertical axis of the graphs the base shear is normalized to the weight of the building, whereas the horizontal axis reports the average displacement of the roof normalized to the height of the building (building drift). The vertical dashed lines indicate the displacement where the base shear capacity in the pushover curves had decayed by 20% (or the last step that reached convergence), considered here as the ultimate displacement d_u of the nonlinear static procedure. In Table 5 a summary of the main results from the numerical analyses is reported: the fundamental period and the corresponding mass participation, the ratio between the maximum base shear normalized to the weight of the building, the yield and ultimate displacement from the pushover analyses obtained by transforming the pushover curves to their bilinear equivalents (as suggested in EN 1998-1), the ductility values derived from the bilinear curves, and the maximum displacement from the dynamic analyses.

In Figure 7 it is observed for AH that in the x direction similar result were obtained from the dynamic and static analyses. This finding is consistent with the damage observed after the earthquake, where the South façade exhibited extensive damage and had probably lost all of its horizontal resistance. In the y direction the building exhibited a lower level of damage, with a comparable extent of damage also implied by the rather narrow loops obtained from the dynamic analysis. In the positive x direction the ultimate displacement for the two load distributions was almost coincident, and in the positive y direction the ultimate displacement d_u for the inverted triangular load pattern corresponds to a drift of 1.08% and is outside the scale for the graph. Finally, in the negative x direction when the uniform load distribution was applied, drift corresponding to 20% decay of shear base occurred at approximately 0.08% (marked by the red dashed line in Figure 7). However this value is not considered as the ultimate displacement because the model regained its strength as lateral displacement further increased. Therefore this value was not reported in Table 5.

RH exhibited less damage after the earthquake that was experienced by AH, and the results of the dynamic hysteresis also show narrow loops that indicate a lower extent of damage. Furthermore the dynamic response exhibits little strength loss, which is another indicator that the building was probably able to support a higher demand.

Table 5. Summary of the main results from numerical analyses

	Dir.	**T_1 [s]**	**$m_X - m_Y$ [%]**	**V_{max}/W**	**d_y [mm]***	**d_u [mm]***	**μ***	**PGA [m/s^2]****	**d_{max} [mm]**
AH	X	0.2	62 – 0	0.17	2.5	42.4	12.0	3.71	36.9
	Y	0.13	0 – 51	0.32	3.1	39.1	12.6	4.06	16.1
RH	X	0.19	48 – 0	0.22	1.8	36.7	19.8	9.03	6.56
	Y	0.17	0.4 – 26	0.33	2.8	16.7	6.00	7.54	4.99

*results refer to the load distribution that showed the lowest ductility: red uniform, blue triangular

**PGA in vertical direction used for the analyses: AH = 6.78 m/s^2, RH = 4.03 m/s^2

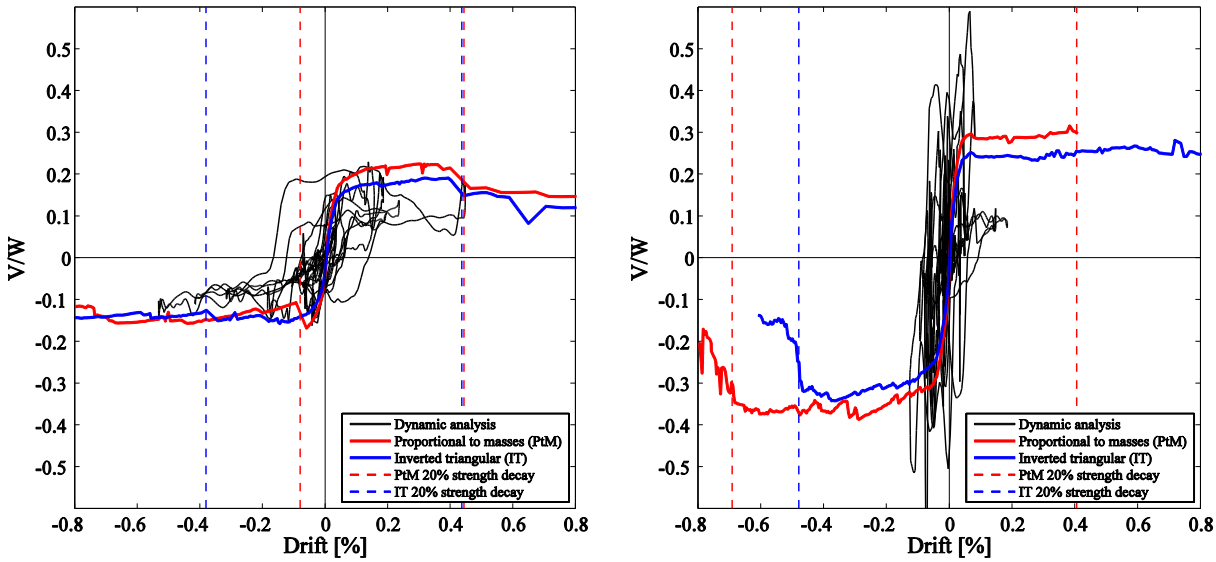

a) X direction b) Y direction

Figure 7 - Comparison of results for pushover analysis and nonlinear time history analysis for AH

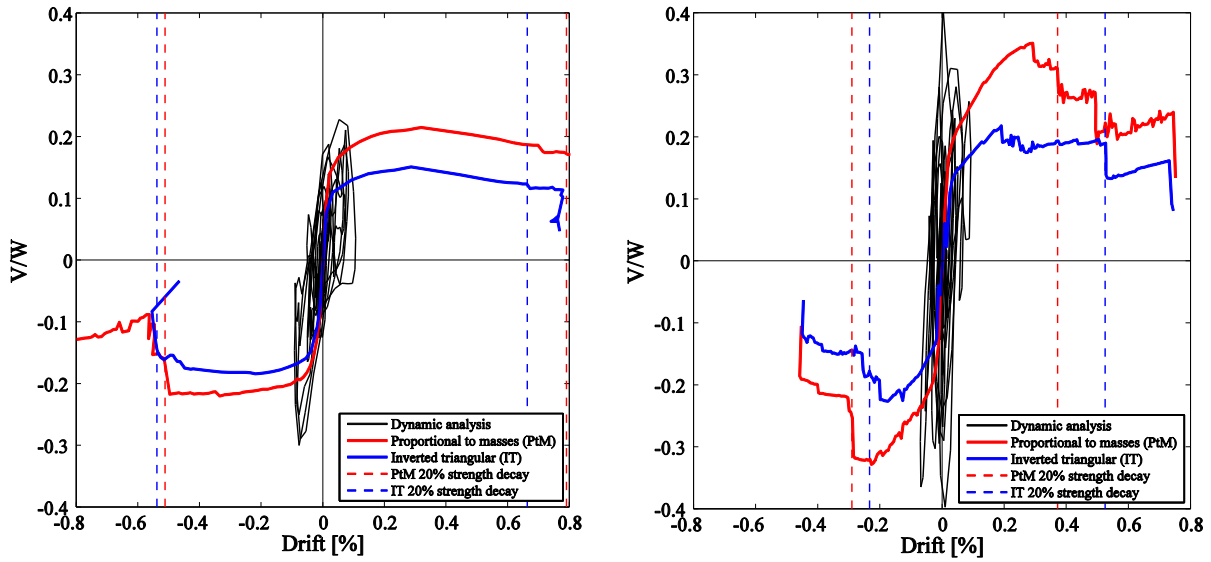

a) X direction b) Y direction

Figure 8 - Comparison of results from pushover analysis and nonlinear time history analysis for RH

4 CONCLUSIONS

Numerical analyses that were undertaken using the equivalent frame approach on two models of URM buildings damaged during the Canterbury earthquake sequence showed that when a good level of knowledge of the construction is reached, this method is able to predict with rather high accuracy the level of damage expected (as shown in Figure 5 and 6). Furthermore this methodology has the advantage that a URM building may be modelled with a low number of elements and enable nonlinear dynamic analyses to be undertaken in a short amount of time.

Although AH was constructed of masonry with a high compressive strength, the building exhibited extensive damage that was slightly overestimated by the numerical analysis, mainly in the spandrels of the East façade. This over-estimation was attributed to a lack of knowledge about the cohesion and the

tensile capacity of the bricks, where the default values proposed in NZSEE (2015) were adopted. For RH the nonlinear dynamic analysis slightly underestimated the real damage, which was possibly explained by recognising that it was not possible to fully account for site effects.

5 ACNOWLEDGEMENTS

The authors acknowledge the Canterbury Geotechnical Database for some of the site investigation data used in this study and the New Zealand GeoNet project (www.geonet.org.nz), its sponsors EQC, GNS Science and LINZ, for providing accelerograms used in this study and the OPUS geotechnical company for the borehole data.

The authors acknowledge the pictures and the information provided by Ross Becker of Becker Fraser Photos and by Althea Kallas.

REFERENCES

Beyer, K. 2012. Peak and residual strengths of brick masonry spandrels, *Engineering Structures*, Vol. 41 533-547

Cattari, S. & Lagomarsino, S. 2013. Masonry structures, pp.151-200, in: Developments in the field of displacement based seismic assessment, Edited by T. Sullivan and G. M. Calvi, Ed. IUSS Press (PAVIA) and EUCENTRE, pp.524, ISBN: 978-88-6198-090-7

Cattari, S., Giongo, I., Marino, S., Lin, Y., Schiro, G., Ingham, J.M. & Dizhur, D. 2015. Numerical simulation of the seismic response of an earthquake damaged URM building, Proc. of the 2015 NZSEE Conference, Rotorua 10-12 April 2015.

Dowrick, D.J. 1998. Damage and intensities in the magnitude 7.8 1931 Hawke's Bay, New Zealand, earthquake, *Bulletin of the New Zealand National Society of Earthquake Engineering*, Vol. 31 (3) 139-162

EN 1998-1. 2004. Eurocode 8: Design of structures for earthquake resistance - Part 1: General rules, seismic actions and rules for buildings. CEN (European Committee for Standardization), Brussels, Belgium

EQ STRUCT. 2015. Exemplar seismic assessment calculations, technical report, Auckland, New Zealand

Giongo, I., Wilson, A., Dizhur, D.Y., Derakhshan, H., Tomasi, R., Griffith, M.C., Quenneville P. & Ingham, J.M. 2014. Detailed seismic assessment and improvement procedure for vintage flexible timber diaphragms, *Bulletin of the New Zealand Society for Earthquake Engineering*, Vol. 47(2) 97-118

Lumantarna, Ronald. 2012. Material Characterisation of New Zealand's Clay Brick Unreinforced Masonry Buildings, *PhD thesis*, University of Auckland.

Lagomarsino, S., Penna, A., Galasco, A. & Cattari, S. 2013. TREMURI program: an equivalent frame model for the nonlinear seismic analysis of masonry buildings, *Engineering Structures*, Vol. 56 1787-1799

Mann, W., Müller, H. 1980. Failure of shear-stressed masonry – An enlarged theory, tests and application to shear-walls. 7th International Symposium on Load-bearing Brickwork, London, UK.

NZSEE 2015. Assessment and Improvement of the Structural Performance of Buildings in Earthquakes - Section 10 Revision. Seismic Assessment of Unreinforced Masonry Buildings. New Zealand Society for Earthquake Engineering, Corrigendum n° 4, 22nd April 2015, ISBN 978-0-473-26634-9

Russell, A.P. & J.M. Ingham. 2010. Prevalence of New Zealand's unreinforced masonry buildings, *Bulletin of the New Zealand Society for Earthquake Engineering*, Vol. 43(3) 182-201

Wotherspoon, L.M., Orense, B.A., Bradley, B.A., Cox, B.R., Wood, C.M & Green, R.A. 2015. Soil profile characterisation of Christchurch central business district strong motion stations, *Bulletin of the New Zealand Society for Earthquake Engineering*, Vol. 48(3) 146-156